Revealing the Backbone Structure of B-DNA from Laser Optical Simulations of Its X-ray Diffraction Diagram

A. A. Lucas,* Ph. Lambin, R. Mairesse, and M. Mathot

Facultés Universitaires Notre-Dame de la Paix, 61 rue de Bruxelles, B5000 Namur Belgium

Figure 1a shows what surely ranks as one of the most celebrated scientific pictures of the 20th century. This is the X-ray diffraction pattern produced by a fiber of DNA as reported by Franklin and Gosling and by Wilkins *et al.* (*1*) in 1953. The picture is said (*2*) to have played a key role in the discovery of the double helical backbone structure of DNA by Watson and Crick, a structure that in turn was essential for their conception of the fundamental base-pairing idea (*3*). Having helped unravel the molecular structure of the genes, the pattern can truly be considered as the Rosetta stone of the genetic language.

The many popular accounts (*2*) of the great discovery do not generally allow one to grasp just why Figure 1a proved so crucial in arriving at the correct structure. The original diffraction papers in the technical literature are accessible only to specialists with a solid foundation in crystallography and diffraction theory. This is unfortunate in view of the central importance of DNA for the teaching of all life sciences. It is as if one had to teach the nuclear structure of atoms without being able to rely on the import of the Rutherford backscattering experiment.

The present paper aims at correcting this situation. We begin by describing the intensity features of Figure 1a and by stating the corresponding structural elements of the DNA backbone that these features reveal. Then we perform optical simulation experiments, using a laser and several diffraction gratings (optical transforms), which explain the fundamental scattering processes leading to the formation of the intensity features in the observed X-ray pattern. These experiments can be easily demonstrated in a science class or by an individual person, at any instructional level from introductory to advanced. Since the DNA backbone supports the base-pair sequence, which constitutes the hereditary message, the present "hands-on" familiarization with the double-helix structure and the way it was discovered should contribute to the public understanding of contemporary DNA developments such as DNA fingerprinting, cloning, and the human genome project.

X-ray Diffraction by B-DNA

A schematic of the diffraction setup used by Franklin *et al.* is shown in Figure 1c. The fiber has been pulled out of a viscous water solution of the sodium salt of DNA. It has the thickness of a hair and contains millions of individual DNA strands aligned roughly in parallel by the pulling process. Owing to a relatively high water content of the fiber, the (negatively charged) DNA filaments are kept apart by water molecules and counterions (solvated Na^+). In this so-called "paracrystalline" state, the interdistance between the DNA helical axes and the relative angular orientations of the molecules around their axes are randomly distributed. The DNA is then in the so-called B conformation, which is the one normally adopted in the conditions of a living cell. Other conformations exist but we will only be concerned here with the B form. A simplified space-filling model of the B conformation of DNA is shown in Figure 1e. One recognizes the two intertwined sugar-phosphate backbones forming a regular outer cage around an irregular succession of flat base pairs stacked horizontally inside of the molecule.

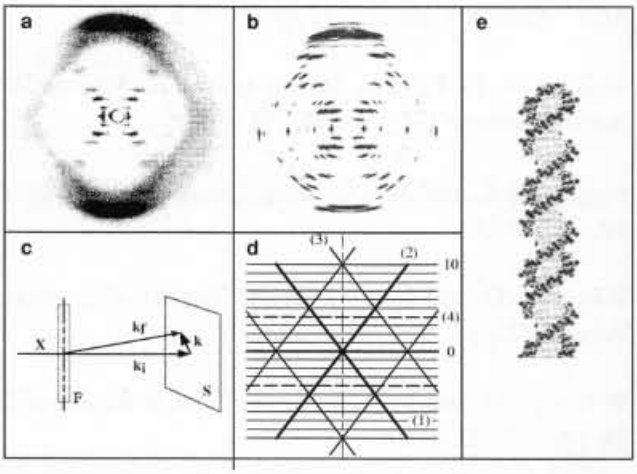

Figure 1. (a) X-ray diffraction fiber diagram from paracrystalline B-DNA (*1*). (b) X-ray diffraction fiber diagram from crystalline B-DNA (*4*). (c) Schematic X-ray diffraction setup: X, X-ray beam; F, DNA fiber; **k**, transfer wave vector; *S*, plane of the diffraction diagram. (d) Schematic intensity features in the fiber diagrams: 1, layer-lines; 2, central X-shaped cross; 3, repeated X-shaped cross producing the diamond pattern; 4, missing 4th layer-line. (e) Model for the B-DNA double helix.

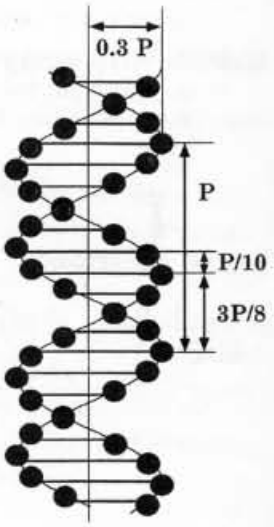

Figure 2. Planar projection of a simplified B-DNA model showing schematically the two helical backbones of spheroidal phosphate groups (circles along the sine waves) and the equidistant planar bases (horizontal bars). The four important dimensions of the molecule are indicated in terms of the double helix period $P = 3.4$ nm.

*Email: *amand.lucas@fundp.ac.be*

We shall also refer to Figure 1b, which reproduces a sharper fiber diagram taken a few years later by Langridge *et al.* (*4*) from a lithium salt of B-DNA in a polycrystalline state. The intensity distributions in Figures 1a,b exhibit several gross characteristics, schematized in Figure 1d. We begin by enumerating these features and by stating, without justifications, the corresponding four geometrical parameters of the molecule that these features imply. It will be the purpose of the optical simulations to explain just how this correspondence is established. The four basic B-DNA dimensions are shown in the schematic double helix of Figure 2.

Layer-Lines: Helix Period P = 3.4 nm (Fig. 2)

By contrast to the sharp, spotty diffraction pattern of a single crystal, the diagrams in Figures 1a,b consist of broad "spots". These smears reflect the partial lateral and orientational disorder of the DNA backbones in the fiber material and also the disorder in the succession of the base pairs. However, the spots are aligned on equidistant horizontal lines called "layer-lines" (the many horizontal lines labeled 1 in Fig. 1d). These are typical of the fiber diagram of straight linear polymers. The layer-line organization is caused by the *periodicity* of the backbone double helix along the molecular axis (the vertical axis in Fig. 1). Measurement of the angular separation between the layer-lines and knowledge of the X-ray wavelength (Cu Kα radiation: $\lambda = 0.15$ nm) reveals the period $P = 3.4$ nm (the numerical value of the layer-line separation is not explicitly stated in the original papers [*1, 4*], but it must have been $\sin\theta \approx \theta = \lambda/P = 0.044$ rad = 2.5°). Although irregular, the succession of the pairs of chemically and structurally different bases A, T, G, C does not destroy the layer-line pattern created by the helical regularity of the backbones.

X-shaped Cross: Helix Radius r = 1 nm (Fig. 2)

Around the center of the picture in Figure 1a, the spots form a prominent cross. This *X-shaped cross* arrangement (labeled 2 in Fig. 1d) is characteristic of the diffraction by a regular helical molecule (*1, 5*). It is this crossed pattern that particularly inspired Crick and Watson in building their successful double helical model. The upper, meridian angle α between the arms of the cross is related to the phosphorus helix radius via the relation $r = (P/2\pi)\cot(\alpha/2)$. The knowledge of P from the layer-lines and the measurement of α reveal the *helix radius* $r = 1$ nm. This relatively large value implies that the sugar-phosphate backbones form a large outer cage inside which the bases are accommodated and point toward the helix axis (Fig. 1e).

Diamond Structure: Interbase Distance d = 0.34 nm (Fig. 2)

The arms of the cross, the big blobs north and south and the east and west ends of the equator layer-line in Figures 1a,b, define four diamond-shaped areas. This "diamond structure" (labeled 3 in Fig. 1d) is caused by the *atomic periodicity* (i.e., the regular succession of the sugar-phosphate groups) of the DNA backbones along the molecular axis (*5*). In the better resolved diagram of Figure 1b, one can count ten layer-line intervals along a vertical diagonal of each diamond, for example from the center of the pattern to the north blob. In keeping with the reciprocity between the real space of the molecule and the reciprocal space of the diffraction pattern, this means that the helix period must be ten times the atomic repeat period of the backbone: the diamond structure reveals an axial *repeat distance* $d = 0.34$ nm between the phosphate groups and therefore also between the successive base pairs (since there is just one base per sugar-phosphate group). Moreover, contrary to the east and west diamonds, the meridian diamonds are devoid of intensity. The latter feature confirms that the sugar-phosphate backbones sit outside and the bases inside of the molecule and not the other way around, as in unsuccessful models proposed before 1953.

Missing 4th Layer-Line: Backbone Separation Δz = 3P/8 (Fig. 2)

When one starts counting the layer-lines from the zeroth equatorial line, one encounters an intensity gap at the nominal position of the 4th layer-line (the broken line labeled 4 in Fig. 1d). This is particularly clear in the better resolved diagram of Figure 1b, although it can also be guessed (*1*) from Figure 1a, where the 5th layer-line reappears strongly. The "missing 4th layer-line" indicates that in the B-form of DNA, the two intertwining coaxial backbones are separated by $3P/8$ along the axis (*1*). This unequal shift of the two backbones creates major and minor grooves in the molecule (Fig. 1e), a peculiar structural feature of B-DNA that has important bearing on the interaction of the molecule with proteins.

All these features can be quantitatively understood from a reference to the standard theory of the diffraction of X-rays by helical molecules, which was developed by Crick and collaborators (*5*) shortly before the momentous discovery of the structure of DNA, and in a different context, for the interpretation of the X-ray pattern produced by polypeptide chains having the α-helical structure proposed by Pauling (see references in *5*). This beautiful theory no doubt played an enormous role in the intellectual path towards the great discovery. However, the mathematical tools used in the theory are again not so elementary as to be easily followed by beginning students or even nonmathematically oriented advanced students or professionals.

To remedy this rather frustrating situation, we designed optical simulations that provide, with no recourse to helical diffraction theory, a qualitative understanding of the origin of the four features, one at a time and clearly separated from each other. Naturally, a quantitative account of the precise and detailed intensity distributions along the layer-lines such as occur in Figure 1b does require full use of the theory (*4*).

Relevance of Planar Models

This section is not required for understanding the optical simulations in the next section and may be skipped altogether by unconcerned readers.

In the optical simulations that follow, the light from a visible laser interacts with planar diffraction gratings on a slide. These gratings represent planar projections of various schematic models of DNA. Although we do not invoke any elaborate theoretical argument, we need to justify (at least in outline) the relevance of such planar gratings in simulating the diffraction by an inherently three-dimensional object such as a helical molecule.

In the first Born approximation, which is generally adequate for X-ray scattering, the intensity elastically scattered by an object is given by the Fourier transform of its electron

density. If the object has its atoms at $\mathbf{r}_j$, the standard intensity expression is

$$|\Sigma_j f_j(\mathbf{k})\exp(i\mathbf{k}\bullet\mathbf{r}_j)|^2$$

where f_j is the atomic scattering factor (i.e., the Fourier transform of the electron density of atom j) and the exponential factor is the Fourier transform of the point-like nuclear density. The Fourier transforms are calculated for a wave vector $\mathbf{k}$, which is the wave vector transferred from the initial to the final scattered X-ray while conserving momentum (Fig. 1c). If the diffraction pattern is recorded at not too large scattering angles, this vector lies nearly in a plane perpendicular to the incident beam direction (Fig. 1c): $\mathbf{k} \approx (0,\mathbf{k}_\perp)$. Then, in the above intensity expression, the only components of $\mathbf{r}_j$ that count in the scalar product $\mathbf{k}\bullet\mathbf{r}_j$ are also the perpendicular components. Hence a 2-D planar diffraction model obtained by projecting all atom positions onto this perpendicular plane will produce about the same forward intensity pattern as the 3-D object.

In the optical simulation experiments described below, the scattering angles are very small indeed (less than 1°) and it would make no difference whatsoever if model 3-D scattering objects were used instead of their 2-D projections onto the plane of the slide. However, for the real X-ray experiment reported in Figures 1a,b, the small-angle approximation is strictly valid not too far from the center of the diagram and is only marginally valid at its periphery: the big blobs north and south occur at a not-so-small angle $\arcsin(\lambda/d) \approx 26°$ from the center of the pattern, since they are caused by the repeat nucleotide distance d = 0.34 nm and with an X-ray wavelength λ of about 0.15 nm. Nevertheless, as we shall see, the optical simulation does fully succeed in reproducing the principal features in the observed X-ray patterns.

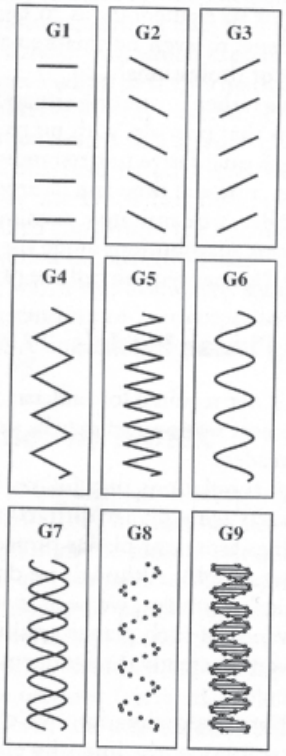

Figure 3. G1–G9: a set of motifs for the nine diffraction gratings used in optical simulation experiments.

Optical Simulations

The use of the optical transform method (i.e. diffraction of visible light from artificial gratings) to simulate X-ray diffraction has a long history. It is probably W. L. Bragg who first suggested the idea (*6*). Successful optical simulations had already been performed before the invention of lasers (*7*). But the advent of highly coherent laser sources, particularly the recent availability of solid-state laser pointers, has made the simulations very much easier. Recently, to simulate the diffraction by inorganic solids, optical transform kits have been developed based on the idea of setting up a "diffraction laboratory on a slide" (*8*). A similar idea independently occurred to us for the present problem of simulating the X-ray diffraction by DNA.

A single standard slide has been prepared containing nine diffraction gratings in 3 ¥ 3 panels. The nine panels were obtained starting from a set of nine vertical periodic motifs, G1–G9, shown in Figure 3. In each panel, the motif is repeated laterally many times in parallel so as to obtain a diffraction grating that fully occupies one-ninth of the slide. The reason for this repetition is to increase the interaction between the laser spot, which has a diameter of several millimeters, and the motif (somewhat as the X-ray beam intercepts many millions of molecules in the DNA fiber used by Franklin *et al.*). The lateral separation between the repeated motifs is randomized to avoid introducing a spurious periodicity and thus to smear out the spots in this lateral direction. A low-resolution photo of the slide is shown in Figure 4, where the nine gratings are labeled G1 to G9 just as in Figure 3.

What was the logical thread followed in the design of the motifs? This is best appreciated on going backward from G9 to G1. The last panel with motif G9 represents a planar projection of the double helix on a plane parallel to the helix axis. Only the phosphates and bases, ten per period, are represented as dots and bars, respectively, as in Figure 2. The phosphate "atoms" are axially equidistant and lie on a sine wave, which represents the planar projection of a regular, circular helix. Inspecting the slide from G9 to G1 makes it

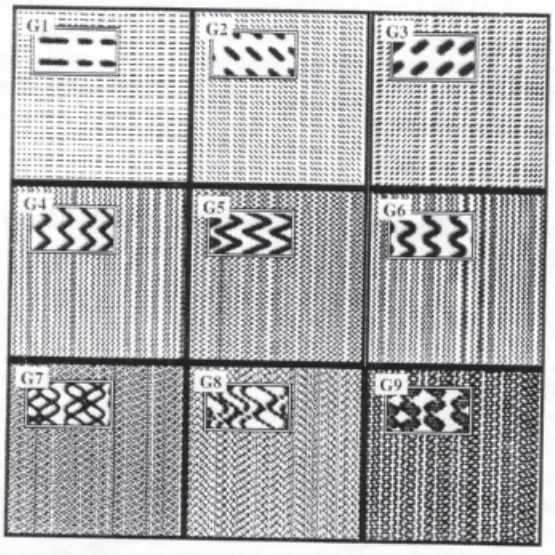

Figure 4. A positive photo of the single slide with the nine diffraction gratings G1–G9. In each grating the basic repeated motif is shown enlarged in the inset.

clear that the final panel was deconstructed step by step in the previous panels by removing structural elements, one at a time. Thus from G9 to G8, one removes the bases and leaves only one atomically resolved sine wave to test the effect of the bases and what kind of pattern is produced by an atomically resolved helix. In G7, the atomicity has been removed to test the effect of having a double helix. The remaining "stripping" is self-evident and ends up in G1 with a simple set of horizontal lines, which usually serve in class for the very first introduction to the diffraction phenomenon.

How did we fabricate the slide? The set of nine gratings is first computer drawn, black-on-white, on a single large sheet of paper. Then the picture is photographed onto a high-resolution film with a size reduction to about 5 parallel motifs per millimeter. (The recent availability of high-resolution computer printing on transparent foils should eliminate this awkward photographic step.) The film negative is then simply mounted on a slide without any protective glass cover, which would cause multiple reflections and blur the diffraction picture. The slide is then ready for the simulations. One simply passes a laser beam successively through the nine panels and projects the diffraction image onto a white screen in a dimmed room. Alternatively, the patterns can also be safely observed by using the much attenuated light reflected from the laser spot on a white screen and looking at the spot through the diffraction gratings held near the eye (*8*). CAUTION: One should never attempt to look directly into the beam itself even with the slide interposed. Finally, as already noted by the authors of ref. *8*, the specially high coherence properties of a laser are not required at all to observe the diffraction patterns of the present DNA slide. In the individual observation method just described, it will suffice to look through the slide at an ordinary point source of light (white or colored) such as a distant flash lamp, a distant street or traffic light, a bright star. One recalls here that similar diffraction phenomena are sometimes produced by street lights seen through window curtains. This mode of observation is particularly suited for the classroom where the use of lasers always remains somewhat hazardous.

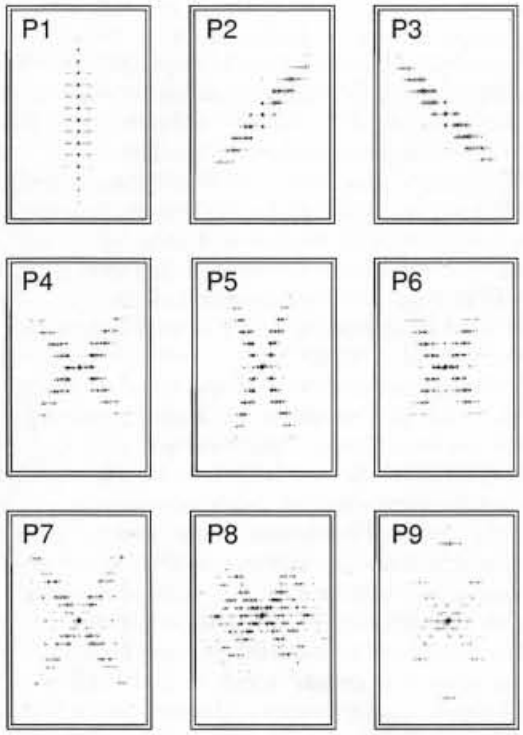

Figure 5. P1–P9: the nine optical diffraction patterns produced by the gratings G1–G9.

The corresponding diffraction patterns are shown in Figure 5, P1–P9.

G1–P1. A set G1 of parallel, equidistant horizontal line segments produces the familiar reciprocal set P1. In order not to confuse the lines on the diffraction slide with the lines of the diffraction pattern, we will refer to the former as "slits". Panel G1 serves as an introductory reminder of the basic *N*-slits diffraction experiment of Thomas Young. The elementary geometrical construction allowing one to grasp the formation of the interference pattern is explained in detail in Figure 6. The scattered light in P1 is segregated along layer-lines. For small scattering angles, the layer-lines are equidistant: their angular separation, seen from the grating, is given by $\sin\theta \approx \theta = \lambda/P$ (see Fig. 6). The z-component of the transfer wave vector is accordingly quantized to $k_z = 2\pi n/P$, where n is an integer numbering the layer-lines (Fig. 6). The intensity maxima of the successive layer-lines are aligned vertically (perpendicular) to the slits. In all nine patterns P1 to P9 and in the X-ray patterns of Figures 1a,b as well, *the layer-line organization reveals the vertical repeat period* P *of the diffracting object.* Such layer-lines always appear, irrespective of the content of the unit cell that is repeated in the vertical direction of each motif.

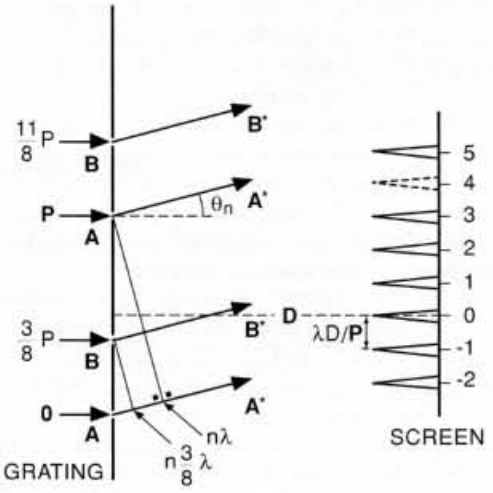

Figure 6. The basic *N*-slits diffraction experiment of Thomas Young. First consider grating A of period P made of slits A alone (in the absence of the B slits): maxima of intensity are sent in directions θ_n so that the successive pairs of rays labeled AA* scattered by the A grating have a path length difference equal to an integer multiple n of wavelengths: $P \sin\theta_n = n\lambda$. On the screen placed at a large distance D from the grating, the intensity maxima (the "layer-lines") are separated by the constant distance $\lambda D/P$. Similarly the B grating of period P considered alone (in the absence of the A slits) would produce exactly the same pattern. However, when considering simultaneously gratings A and B separated by $3P/8$, the triangular construction shown on the exit side of the grating indicates that neighboring rays AA* and BB* have a path length difference of $n3\lambda/8$. For $n = 4$, this amounts to $3\lambda/2$, i.e., the two rays are out of phase and destroy each other on the 4th layer-line (broken line on the screen). The other layer-lines acquire variable intensities (not shown).

What the actual content of the unit cell determines is the horizontal distribution of intensity along each layer-line. If one designates by S the layer-line separation on the screen and by D the distance from slide to screen, then the period P is measured by $P = \lambda D/S = \lambda/\theta$.

G2–P2. A "zig" grating G2 made of equidistant slits rotated clockwise from the horizontal direction produces pattern P2. The layer-line organization persists as it should. But the maxima of intensity now fall along a direction also rotated clockwise by the same angle (i.e., again perpendicular to the inclined slits). One way to understand this slanting effect is to imagine that each individual slit is composed of a set of symmetric pairs of scattering points equidistant from the slit center: each pair acts as a Young two-hole system, which sends a maximum of light intensity in a direction perpendicular to the slit.

G3–P3. A "zag" grating G3 gives P3, obviously the mirror image of G2–P2 with respect to the vertical axis.

G4–P4. A "zigzag" grating G4 produces P4, a combination of P2 and P3. Note the prominent X-shaped cross. The arms of the cross are perpendicular to the directions of the zigzag slits and therefore form an angle α equal to the angle between the zig and the zag. From this, one can measure the ratio a/P of amplitude a to period P of the zigzag, which is about 0.45 in G4 (see Fig. 7).

G5–P5. Another zigzag grating G5 with a *larger* r/P ratio results in an X-shaped cross P5 with a *smaller* opening angle. This is intended to verify visually the relationship between the zigzag amplitude a and the cross opening angle α. Measurement of the latter reveals the value $a/P = (1/4)\text{cotan}(\alpha/2)$ (see Fig. 7). Mathematically inspired students can work out the exact distribution of scattered intensity by calculating the 2-D Fourier transform of a zigzag line, a standard exercise involving elementary integrals.

G6–P6. A continuous sine wave grating G6 produces a pattern P6 that is quite similar to P4: smoothing out the sharp points of the zigzag does not eliminate the basic X-shaped pattern. The ratio r/P of amplitude to period is about 0.3, as for the planar projection of the DNA phosphorus helix (Fig. 2). This demonstrates that the cross in the X-ray pictures (Figs. 1a,b) is caused by the sinusoidal zigzag pattern of the helical DNA backbones projected onto a plane perpendicular to the beam axis (as in Fig. 1e and Fig. 2). From the fact that the arms of the cross are perpendicular to the straight portions of the sine wave (around its inflection points), one can easily deduce, from elementary trigonometry, the ratio $r/P = (1/2\pi)\ \text{cotan}\ \alpha/2$ (see Fig. 7). Note also that there is no intensity within the meridian angles α of the cross.

It is not the first time that the optical transform of a sine wave is shown to resemble the cross-shaped X-ray pattern of B-DNA (*9*). However, the present simulation G1–G6 shows just how the cross is generated—namely, from scattering by the nearly "straight" portions of the sine wave projections of the DNA helices. This is indeed where most of the curvilinear length and therefore scattering power of the motif resides. In addition, the simulation makes it clear that a similar cross will arise from essentially any zigzagging linear motif, not necessarily of sinusoidal form. For example, using a laser pointer the reader can verify that the optical transform of a piece of nylon stocking or other finely woven fabric also produces the characteristic X-shaped pattern (choose one in which the threads are woven in a submillimeter zigzag pattern).

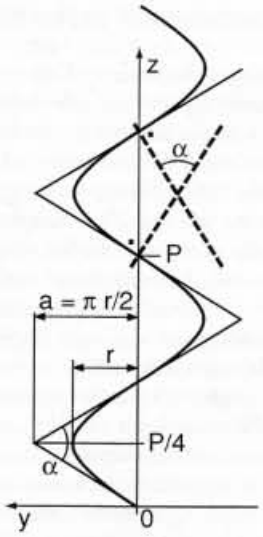

Figure 7. A sine wave motif and its associated zigzag motif whose zig and zag segments are tangent to the sine wave at its inflection points (0, $P/2$, P, ...). The optical transforms of these motifs show a prominent X-shape cross (see Fig. 4, P4–P6) whose arms are perpendicular to the zig and zag segments (broken lines). The upper angle α of the cross is given via the slope of the first zig segment: cotan $\alpha/2 = 4a/P$. The sine wave equation $y = r \sin(2pz/P) \approx r\,2pz/P$ written for small z and compared to the zig equation $y = 4az/P$ identifies the sine amplitude $r = 2a/p$.

G7–P7. Instead of a single sine wave, the repeated motif G7 consists of a pair of coaxial sine waves displaced with respect to each other by the constant axial shift $\Delta z = 3P/8$ (or, equivalently, $\Delta z = 5P/8$, the complement to a full period P). The two sine waves represent the projections of the two sugar-phosphate backbones of B-DNA (Fig. 2). This motif produces P7. Note the layer-lines, the cross, and, most spectacular, the extinction of the 4th layer-line. This is caused by destructive interference between the radiations scattered by the two axially shifted sine waves: along the $n = 4$ layer-line, the rays scattered by the two sine waves arrive with a phase shift $\Delta z \cdot 2\pi n/P = 3\pi$ (i.e., out of phase) and therefore cancel each other. This cancellation is pictorially explained by Figure 6 for the simple case of the interference pattern produced by the basic slit setup of Thomas Young. The reasoning is immediately transposable to a diffraction grating of any shape, such as the double sine wave. Indeed, any arbitrary pair of identical motifs axially displaced by $3P/8$ can be considered as being fully made up of subsets of points or slits, each subset having the geometry of Figure 6 and therefore producing no intensity on the 4th layer-line.

Note that a separation of $\Delta z = P/8$ (equivalently $\Delta z = 7P/8$) would also extinguish the 4th layer-line but such a shift is impossibly small in the real molecule for obvious steric reasons. The absence of the 4th layer-line in the diffraction patterns of Figures 1a,b therefore indicates that the two strands of the backbone of DNA in its B conformation are axially separated by $3P/8$.[1]

If the separation of the double sine wave were $\Delta z = P/2$, then the phase shift would be $n\pi$, leaving nonzero intensity only on the even number layer-lines $n = 0$, 2, 4, 6, and 8. The extinction of the odd layer-lines in effect doubles the layer-line distance, which of course corresponds to the halving of the period of the double sine wave motif in this case. This situation would have applied to DNA if its two strands had been axially separated by $P/2$ and had run in the same direction (a discussion of this point is enacted in the film *Life Story* produced by the BBC *Horizon* program). Instead they are counter-oriented,[1] which in itself suffices to break the $P/2$ translational symmetry and restore the odd layer-lines. In the B conformation, the symmetry is further strongly broken by the unequal $3P/8$ separation.

G8–P8. In this panel we go back to a single sine wave motif as in G6; but this time, the sine wave is "atomized" into 10 dots per period. These dots are axially equidistant and simulate the phosphate groups of atoms in one of the two DNA helices. Note the diamond pattern in P8. The vertical diagonals of the diamonds span 10 layer-line intervals. As Figure 1d suggests, the pattern emerges from repeating the central cross along the vertical axis every 10 layer-lines (*5*) (with due allowance for increased attenuation at large transfer wave vectors). Such a repeat in the diffraction pattern is a necessary consequence of the presence of a new repeat distance in the diffracting object. Note also the absence of intensity in the meridian (north and south) diamonds. In the real molecule, atomic helices made of identical atoms pertaining, say, to the sugar groups are placed inside of the phosphate backbones (i.e., they have a smaller r/P ratio) and hence scatter intensity into more opened crosses sitting outside of the phosphate meridian diamonds (compare the G4-G5 simulations). Hence the absence of intensity in the meridian diamonds of Figure 1b corroborates the exterior position of the backbones.

G9–P9. A double atomically resolved sine wave grating, 10 "atoms" per period, $3P/8$ axial shift, produces P9. A set of 10 horizontal bars connecting the two sine waves roughly model the DNA base pairs. This panel, which encompasses the previous ones, is quite reminiscent of Figures 1a,b. The simple model "bases" correctly reinforce the meridian spots north and south of the pattern. In the real molecule, the large number of atoms in the irregular base pairs are in a somewhat disordered arrangement, which forms no regular helices. However because the bases are flat and regularly spaced every 0.34 nm, these atoms make a large contribution to the big intensity blobs north and south of the diffraction picture.[2]

Conclusion

We have simulated the X-ray diffraction pattern of B-DNA by means of laser optical transforms of planar gratings. These were designed to progressively simulate the effect on the diffraction pattern produced by each of the four invariant structural parameters of the molecule. The demonstrations use an absolute minimum of equipment: a laser and a single slide (available from the authors on request).[3] No other "optics" is required. By simply holding a laser pointer in one hand and the slide in the other, anyone can reproduce the simulation practically anywhere by projecting the diffraction picture on a white wall a few meters away. The demonstration works even in broad daylight when the pattern is projected in a dark corner. For a large audience (more than about 50 persons) a 10-mW He-Ne laser in a dimmed auditorium is preferable (when authorized by safety regulations) and can produce large, clearly visible patterns several tens of meters away. The simulations illustrate several concepts in the diffraction phenomenon and provide an opportunity to discuss the geometrical and atomic structures of DNA, the most beautiful and most important of all molecules of life.

Acknowledgments

We are grateful for the partial support of the Interuniversity Research Program on Reduced Dimensionality Systems (PAI/IUAP 4/10) initiated by the Belgian Government.

One of us (A.A.L.) is grateful to H. Kroto for organizing the videotaping of the optical demonstration in the framework of the VEGA Science Trust, Reflections on Science series. Information on this and other videotapes can be obtained at *http://www.vega.org.uk*. We thank most sincerely Arthur Ellis and George Lisensky for their considerable help kindly provided to improve the manuscript.

Notes

1. The backbone structure of the real B-DNA molecule has a twofold symmetry axis such that one 5′,3′ oriented sugar-phosphate backbone transforms into the other, counter-oriented backbone upon the 180° C-2 rotation (*3*). Thus one sugar-phosphate backbone cannot derive from the other by any axial translation. However, the Δz translation operation used here for the simulation is a genuine symmetry operation for the spheroidal phosphate groups of atoms alone, which happen to dominate the X-ray scattering on account of their large electron density.

2. The reader might wonder why the pattern of Figure 1b is not completely north–south symmetrical as it should for the perpendicular diffraction geometry of Figure 1c: for example, the 0.34 nm north blob is stronger than the south one. This was caused by a slight tilting of the DNA fiber away from the normal to the X-ray beam in order to bring the flat bases closer to the Bragg reflection angle in the upper part of the pattern.

3. The optical transform procedure for simulating DNA diffraction is being developed as an educational kit to complement an existing Optical Transform kit. Both kits are available from the Institute for Chemical Education (email: *ice@chem.wisc.edu;* URL: *http://ice.chem.wisc.edu*) beginning in April 1999.

Literature Cited

1. Franklin, R. E.; Gosling, R. G. *Nature* **1953**, *171*, 740. Wilkins, M. H. F.; Stokes, A. R.; Wilson, H. R. *Nature* **1953**, *171*, 738.
2. A balanced view of the events leading to the discovery can be obtained by reading a number of popular accounts, among which are: Watson, J. D. *The Double Helix*; Atheneum: New York, 1968. Sayre, A. *Rosalind Franklin and DNA*; Norton: New York, 1975. Judson, H. F. *The Eighth Day of Creation*; Penguin: New York, 1979. Crick, F. H. C. *What Mad Pursuit*; Basic Books: New York, 1988.
3. Watson, J. D.; Crick, F. H. C. *Nature* **1953**, *171*, 737.
4. Langridge, R.; Seeds, W. E.; Wilson, H. R.; Hooper, C. W.; Wilkins, M. H. F.; Hamilton, L. D. *J. Biophys. Biochem. Cytol.* **1957**, *3*, 767.
5. Cochran, W.; Crick, F. H. C.; Vand, V. *Acta Crystallogr.* **1952**, *5*, 581.
6. Harburn, G.; Taylor, C. A.; Welburry, T. R. *Atlas of Optical Transforms*; G. Bell & Sons: London, 1975.
7. Hooper, C. W.; Seeds, W. E.; Stokes, A. R. *Nature* **1955**, *175*, 681.
8. Lisensky, G. C.; Kelly, T. F.; Neu, D. R.; Ellis, A. B. *J. Chem. Educ.* **1991**, *68*, 91 and references therein.
9. Welberry, T. R.; Thomas, J. M. *Chem. Br.* **1989**, *25*, 383.